

Perturbation Theory of Single Particle Spectrum of Antiferromagnetic Mott Insulating States in the Hubbard Models

Wenxin Ding^{1*}, Rong Yu^{2,3}

¹*School of Physics and Optoelectronic Engineering,
Anhui University, Hefei, Anhui Province, 230601, China*

²*Department of Physics and Beijing Key Laboratory of Opto-electronic Functional Materials & Micro-nano Devices,
Renmin University of China, Beijing 100872, China*

³*Key Laboratory of Quantum State Construction and Manipulation (Ministry of Education),
Renmin University of China, Beijing, 100872, China*

(Dated: October 31, 2023)

In this work, we present an analytical framework for studying antiferromagnetic (AFM) Mott insulating states in the Hubbard model. We first derive an analytical solution for the single-particle Green's functions in the atomic limit. Within a second-order perturbation approach, we compute the ground state energy and show that the ground state is antiferromagnetically ordered. Then we derive an analytical solution for single-particle Green's functions when effects of the hopping term are considered in the Néel state. With the analytical solution, we compute and explain various properties of antiferromagnetic Mott insulators observed both experimentally and numerically: i) magnetic blueshift of the Mott gap; ii) spectral functions with features comparable to observations by angle-resolved photoemission spectroscopy on parental compounds of cuprate high T_c superconductors. This work comprehends the electronic properties of antiferromagnetic Mott states analytically and provides a foundation for future investigations of doped antiferromagnetic Mott insulators, aiming for the mechanism of cuprates high- T_c superconductivity.

The mechanism of high T_c superconductivity in cuprates[1] is one of the most challenging problems in modern condensed matter physics. Although they are generally three-band, charge transfer insulators[2], it is widely accepted that the mechanism is rooted in the physics of doped antiferromagnetic (AFM) Mott insulators[3], which can be adequately described by single band Hubbard models (HM)[4, 5] with a large onsite repulsion U .

However, despite its seemingly simplicity, we still do not have a well-controlled and comprehensive analytic theory for the strong coupling limit of the HM, except for some aspects of its properties. For example, the AFM order at half-filling was long established through the superexchange mechanism [6]. But incorporation of antiferromagnetism within a systematic solution of HM on equal footing with charge dynamics, often through slave particle constructions[7–11], appears to be difficult and remains unsolved to this day. Lacking a proper theory for AFM Mott states hinders further study for the doped cases. In fact, even theoretical understanding for single[12, 13] or a few impurities[14] proves to be difficult in the absence of such a theory.

The common difficulties encountered in previous works are i) noncanonical operator algebras and ii) lack of Wick's theorem. Both make perturbation sequence difficult to control. Recently, Shastry group pioneered a series of works studying the $t - J$ model[15], the *extremely correlated Fermi liquid* (ECFL) theory[16, 17], and obtained results quantitatively comparable to numerical methods such as dynamical mean field theories[18] and density matrix renormalization

group[19]. ECFL overcomes these difficulties by combining the noncanonical algebras with Heisenberg-equations-of-motion (HEOM) to derive a close-form Schwinger-Dyson-equations-of-motion (SDEOM) for the dynamical Green's functions (GFs). W. Ding further generalized the ECFL idea to arbitrary operators and many-body correlations[20].

In this work, we develop a self-contained and analytic treatment of the HM in the large- U limit at half-filling. We first solve the atomic HM at a single site exactly. With the atomic limit solution, we perform a second-order dynamical and perturbative calculation of the ground state energy to show that the lattice ground state is antiferromagnetically ordered. Then we derive an analytic solution for single-particle GFs in such AFM Mott states of the HM on a square lattice with only nearest neighbor (nn) hopping. Finally, we study the physical properties through the single-particle GFs and compare with previous numerical studies and experimental observations. Through such comparison, we demonstrate that our analytic theory provides an accurate and efficient description for the AFM Mott insulating states of the HM.

Model and Methods.— In this work, we study the HM[4] in the large- U limit. We use *complete operator basis sets* (COBS) [21, 22] to realize a complete description of interacting quantum systems. A COBS is the complete collection of orthogonal operators $\{\hat{u}^\alpha\}$ of the system. The many-body $\{\hat{u}^\alpha\}$ can be constructed from a local COBS $\{\hat{u}_i^\alpha\}$ as tensor products. The orthogonality is defined by the inner product $(\hat{u}^\alpha, \hat{u}^\beta) = \text{Tr}(\hat{u}^\alpha, \hat{u}^\beta) = C\delta_{\alpha\beta}$, where C is typically chosen to be 1. The complete-

ness requires the algebra of COBS to be closed: $[\hat{u}^\alpha, \hat{u}^\beta] = \sum_\gamma b_\gamma^{\alpha\beta} \hat{u}^\gamma$, $\{\hat{u}^\alpha, \hat{u}^\beta\} = \sum_\gamma f_\gamma^{\alpha\beta} \hat{u}^\gamma$, where bs and fs are structure constants. With the orthogonality and completeness, any operators, most notably the density operator $\hat{\rho}$, can be expanded in terms of COBS as $\hat{\rho} = \sum_\alpha \langle \hat{u}^\alpha \rangle \hat{u}^\alpha$.

Locally, we need the following COBS to describe an atomic limit state: i) the single particle operators $\hat{c}_{\sigma i}, \hat{c}_{\sigma i}^\dagger, \hat{\eta}_{\sigma i} = \hat{n}_{\sigma i} - 1/2$, ii) the electronic spin operators $\hat{s}_i^\alpha = \hat{c}_{i\alpha}^\dagger \sigma_{ab} \hat{c}_{ib}/2$, iii) the local vertex operators $\hat{v}_{\sigma i}^\dagger = \hat{c}_{\sigma i}^\dagger \hat{\eta}_{\sigma i}$, $\hat{v}_{\sigma i} = \hat{c}_{\sigma i} \hat{\eta}_{\sigma i}$, iv) the double fermion creation/annihilation operators $\hat{c}_{i\uparrow}^\dagger \hat{c}_{i\downarrow}^\dagger$, $\hat{c}_{i\uparrow} \hat{c}_{i\downarrow}$ and v) the double occupancy operator $\hat{D}_i = \hat{\eta}_{i\uparrow} \hat{\eta}_{i\downarrow}$. For nonlocal correlations, we shall expand the list as needed. Then in our notation, the HM at exact half filling is defined by the Hamiltonian

$$\mathcal{H} = \mathcal{H}_U + \mathcal{H}_t, \quad (1)$$

where $\mathcal{H}_U = U \sum_i \hat{D}_i$ and $\mathcal{H}_t = - \sum_{ij} t_{ij\sigma} \hat{c}_{i\sigma}^\dagger \hat{c}_{j\sigma}$.

In the atomic limit, for a half-filled state, we only need to consider $\langle \hat{s}_i^z \rangle_0 = \pm 1/2$ as the atomic building blocks. Throughout this work, we use the subscript $_0$ to denote atomic limit values. Other spin orientations can be rotated to \hat{z} -direction due to the $SU(2)$ symmetry. Also, at half-filling $\langle \hat{\eta}_{i\uparrow} \rangle_0 = -\langle \hat{\eta}_{i\downarrow} \rangle_0 = \langle \hat{s}_i^z \rangle_0$. Therefore, we only need to consider a product state $|\Psi\rangle = \otimes_i |\langle \hat{s}_i^z \rangle_0\rangle$ with $\langle \hat{s}_i^z \rangle_0 = \pm 1/2$. Note that in the atomic limit, we cannot have a paramagnetic pure state.

To study the system dynamically, we introduce the usual time-ordered dynamical correlation functions, or simply GFs, between elements of COBS: $iG_\pm[\hat{u}^\alpha(t_i), \hat{u}^\beta(t_f)] = \langle\langle \mathcal{T}_\pm(\hat{u}^\alpha(t_i), \hat{u}^\beta(t_f)) \rangle\rangle$, where \mathcal{T}_\pm denotes time-ordering with the \pm sign, $\langle\langle \rangle\rangle$ denotes fully dynamical correlations defined as $\langle\langle \hat{u}^\alpha(t_i) \hat{u}^\beta(t_f) \rangle\rangle = \langle(\hat{u}^\alpha(t_i) - \langle \hat{u}^\alpha \rangle)(\hat{u}^\beta(t_f) - \langle \hat{u}^\beta \rangle)\rangle$. For a given state, $G_\pm[\hat{u}^\alpha(t_i), \hat{u}^\beta(t_f)]$ can be solved from the HEOM and SDEOM: $i\partial_t G_\pm[\hat{u}^\alpha(t_i), \hat{u}^\beta(t_f)] = \langle[\hat{u}^\alpha, \hat{u}^\beta]_\mp\rangle + \sum_{\gamma\eta} h_\eta b_\eta^{\alpha\gamma} \hat{u}^\gamma G_\pm[\hat{u}^\gamma(t_i), \hat{u}^\beta(t_f)]$, in principle. The number of COBS would increase exponentially in practice. Therefore, we need to restrain the calculation to the minimal closed set of SDEOM with controlled approximations. In this work, we shall focus on the single-particle fermionic GFs, $G_-[\hat{c}_{\sigma_i x_i}, \hat{c}_{\sigma_f x_f}^\dagger]$, where x_i and x_f denote the lattice coordinates of the operator at initial and final times. We also omit the time label unless noted otherwise.

Atomic GFs.– To obtain a set of solvable equations for $G_-[\hat{c}_{\sigma_i x_i}, \hat{c}_{\sigma_f x_f}^\dagger]$, the key step is to identify the spectral generating algebra (SGA)[23] for $\mathcal{H}_{U,i} = U \hat{D}_i$. We find that

$$\begin{aligned} [\hat{D}_i, \hat{c}_{\sigma i}] &= -\hat{v}_{\sigma i}, & [\hat{D}_i, \hat{c}_{\sigma i}^\dagger] &= \hat{v}_{\sigma i}^\dagger, \\ [\hat{D}_i, \hat{v}_{\sigma i}] &= -\hat{c}_{\sigma i}/4, & [\hat{D}_i, \hat{v}_{\sigma i}^\dagger] &= \hat{c}_{\sigma i}^\dagger/4, \end{aligned} \quad (2)$$

which form the minimal set of a closed SGA. Accordingly, we take the time derivative twice. Given an atomic state, we find

$$\begin{aligned} -\partial_t^2 G_-[\hat{c}_{\sigma_i x_i}, \hat{c}_{\sigma_f x_f}^\dagger] &= (\delta'(t) - \sigma_i \delta(t) U \langle \hat{s}_i^z \rangle_0) \\ &\times \delta_{\sigma_i \sigma_f} \delta_{x_i x_f} + \frac{U^2}{4} G_-[\hat{c}_{\sigma_i x_i}, \hat{c}_{\sigma_f x_f}^\dagger], \end{aligned} \quad (3)$$

where we used $\langle\langle \hat{c}_{\sigma_i x_i}, \hat{c}_{\sigma_f x_f}^\dagger \rangle\rangle_0 = \delta_{\sigma_i \sigma_f} \delta_{x_i x_f}$ and $\langle\langle \hat{v}_{\sigma_i x_i}, \hat{c}_{\sigma_f x_f}^\dagger \rangle\rangle_0 = \langle \hat{\eta}_{\sigma_i} \rangle_0 = -\sigma_i \langle \hat{s}_i^z \rangle_0$ with a sign convention $\sigma = +$ when $\sigma = \uparrow$ and $\sigma = -$ when $\sigma = \downarrow$. We simplify the results in frequency space as

$$G_-[\hat{c}_{\sigma_i x_i}, \hat{c}_{\sigma_f x_f}^\dagger] = \delta_{x_i x_f} \delta_{\sigma_i \sigma_f} \frac{\omega - \sigma_i U \langle \hat{s}_i^z \rangle_0}{\omega^2 - U^2/4}. \quad (4)$$

Before we proceed to the next part, we point out an important character of the atomic GFs. The $|\uparrow\rangle$ state can only be excited by \hat{c}_\uparrow or $\hat{c}_\downarrow^\dagger$, not the other way around. In terms of the GFs, we find that $\langle \hat{s}_i^z \rangle_0 = 1/2$, we find $G_-[\hat{c}_{\sigma_i x_i}, \hat{c}_{\sigma_f x_f}^\dagger] = (\omega + U/2)^{-1}$ and for $\langle \hat{s}_i^z \rangle_0 = -1/2$ $G_-[\hat{c}_{\sigma_i x_i}, \hat{c}_{\sigma_f x_f}^\dagger] = (\omega - U/2)^{-1}$. Therefore, there is only one pole with nonzero spectral weight in the atomic limit, which corresponds to either the upper or lower Hubbard band (UHB or LHB). Such behavior also can be viewed as a Luttinger “surface” or GF zeros[24, 25] in the atomic limit. We shall find this character still manifesto in the spin-projected GFs of the lattice case.

Algebraic generation of perturbation sequences.– Traditionally, dynamical perturbation expansion relies on the validity of Wick’s theorem thus only applies to canonical operators with a Gaussian “free” state. Systematic generation of perturbation sequences in a strong coupling limit, such as for the HM[26, 27], remains a challenging problem. Within the Hamiltonian and SDEOM approach of this work, the dynamical perturbation sequence on an arbitrary “free” state can be generated algebraically through higher orders of time derivatives for the operators and GFs, following Schwinger’s construction of action principle [28]. For the current problem, we need the second order HEOM

$$\begin{aligned} \frac{\partial^2}{\partial t^2} \hat{O} &= -\frac{1}{2!} \left([[\mathcal{H}_t, \mathcal{H}_U], \hat{O}] + [\mathcal{H}_t, [\mathcal{H}_t, \hat{O}]] \right. \\ &\quad \left. + [\mathcal{H}_t, [\mathcal{H}_U, \hat{O}]] + [\mathcal{H}_U, [\mathcal{H}_U, \hat{O}]] \right), \end{aligned} \quad (5)$$

where \hat{O} is an arbitrary operator of interest. Eq. (5) is exact. When Eq. (5) is applied to GFs of \mathcal{H}_U , it generates the second order dynamical perturbation due to \mathcal{H}_t . Let $\hat{O} = \hat{c}_{\sigma_i}$, we obtain the dynamical perturbation terms for $G_-[\hat{c}_{\sigma_i x_i}, \hat{c}_{\sigma_f x_f}^\dagger]$.

Magnetic energy from perturbation.– Next, we employ Eq. (5) to prove within the current framework that the spins should be antiferromagnetically aligned. To achieve that, we compute the expectation value of

the nn hopping term $\langle \hat{c}_{\sigma_i}^\dagger \hat{c}_{\sigma_{i+1}} \rangle = -\langle \hat{c}_{\sigma_{i+1}} \hat{c}_{\sigma_i}^\dagger \rangle$ perturbatively to the second order. We compute via the relation $\langle \hat{c}_{\sigma_i} \hat{c}_{\sigma_j}^\dagger \rangle = iG_-[\hat{c}_{\sigma_i}, \hat{c}_{\sigma_j}^\dagger](t=0^+)$.

By inspecting the operator algebras, we find the lowest order nonzero correction to be $-\partial_t^2 G_-[\hat{c}_{\sigma_i}, \hat{c}_{\sigma_j}^\dagger] = -tU \langle \hat{\eta}_{\bar{\sigma}_i}^z \rangle G_{-,0}[\hat{c}_{\sigma_j}, \hat{c}_{\sigma_j}^\dagger]$. The correction comes from $[H_t, [H_U, \hat{c}_{\sigma_i}]]$ of Eq. (5). Plug in the results of (3), we find $\langle \hat{c}_{\sigma_i} \hat{c}_{\sigma_j}^\dagger \rangle = -\frac{t}{U} \langle \hat{\eta}_{\bar{\sigma}_i}^z \rangle_0 \langle \hat{\eta}_{\sigma_j}^z \rangle_0$. Again, use $\langle \hat{\eta}_{\sigma_i}^z \rangle = -\langle \hat{\eta}_{\bar{\sigma}_i}^z \rangle = \langle \hat{s}_i^z \rangle$ and the correction to energy per bond is $\Delta E = \frac{4t^2 \langle \hat{s}_i^z \rangle_0 \langle \hat{s}_j^z \rangle_0}{U}$. The sign shows that $\langle \hat{s}_i^z \rangle_0$ aligned in an AFM pattern is energetically more favorable when subject to the perturbation of \mathcal{H}_t . The amplitude $4t^2/U$ is consistent with previous results through the superexchange mechanism[6, 11]. For previous works in the strong coupling limit[3, 7–10], capturing magnetism consistently is a unmet challenge until the current work.

Second order theory from product Néel states.– In this part, we solve for $G_-[\hat{c}_{\sigma_i x_i}, \hat{c}_{\sigma_f x_f}^\dagger]$ at the second order on top a product AFM Néel state. However, we must emphasize that the AFM Néel state is still two-fold degenerate. A more rigorous calculation requires parameterization of the two-fold degeneracy before the perturbation. We restrict to the product state for a simpler demonstration.

Consider the full SDEOM up to the second order time-derivative:

$$\begin{aligned} \omega^2 G_-[\hat{c}_{\sigma_i}, \hat{c}_{\sigma_f}^\dagger] &= \omega \delta_{x_i, x_f} \delta_{\sigma_i, \sigma_f} \\ &+ U \omega G_-[\hat{v}_{\sigma_i}, \hat{c}_{\sigma_f}^\dagger] - \sum_j t_{ij} \omega G_-[\hat{c}_{\sigma_i, j}, \hat{c}_{\sigma_f}^\dagger] \end{aligned} \quad (6)$$

$$\begin{aligned} \omega G_-[\hat{v}_{\sigma_i}, \hat{c}_{\sigma_f}^\dagger] &= -\sigma \langle \hat{s}_i^z \rangle_0 \delta_{x_i, x_f} \delta_{\sigma_i, \sigma_f} \\ &+ U/4 G_-[\hat{c}_{\sigma_i}, \hat{c}_{\sigma_f}^\dagger] - \sum_j t_{ij} (G_-[\hat{\eta}_{\bar{\sigma}_i}^z \hat{c}_{\sigma_i, j}, \hat{c}_{\sigma_f}^\dagger] \\ &+ G_-[\hat{s}_i^+ \hat{c}_{\sigma_i, j}, \hat{c}_{\sigma_f}^\dagger] - G_-[\hat{c}_{\sigma_i, j}^\dagger \hat{c}_{\sigma_i} \hat{c}_{\bar{\sigma}_i}, \hat{c}_{\sigma_f}^\dagger]), \end{aligned} \quad (7)$$

where the unperturbed values are used for static correlations.

To obtain closed equations, we make further approximations on the new GFs generated in Eq. (8). First, we argue that we can simply ignore both $G_-[\hat{s}_i^+ \hat{c}_{\sigma_i, j}, \hat{c}_{\sigma_f}^\dagger]$ and $G_-[\hat{c}_{\sigma_i, j}^\dagger \hat{c}_{\sigma_i} \hat{c}_{\bar{\sigma}_i}, \hat{c}_{\sigma_f}^\dagger]$. $G_-[\hat{s}_i^+ \hat{c}_{\sigma_i, j}, \hat{c}_{\sigma_f}^\dagger]$ is the coupling between single electron excitations and AFM spin fluctuations, which is apparently a higher order effect. The lowest order and dominating effect should be the AFM order, not its fluctuations. $G_-[\hat{c}_{\sigma_i, j}^\dagger \hat{c}_{\sigma_i} \hat{c}_{\bar{\sigma}_i}, \hat{c}_{\sigma_f}^\dagger]$ can be estimated as $\langle \hat{c}_{\sigma_i, j}^\dagger \hat{c}_{\bar{\sigma}_i} \rangle G_-[\hat{c}_{\sigma_i}, \hat{c}_{\sigma_f}^\dagger]$ near the atomic limit, which is a self-iteration of the single-particle GFs hence also a higher order term.

Therefore, we are left with the non-local vertex function $G_-[\hat{\eta}_{\bar{\sigma}_i}^z \hat{c}_{\sigma_i, j}, \hat{c}_{\sigma_f}^\dagger]$ which we approximate in a

Hartree[29] way

$$G_-[\hat{\eta}_{\bar{\sigma}_i}^z \hat{c}_{\sigma_i, j}, \hat{c}_{\sigma_f}^\dagger] \simeq \langle \hat{\eta}_{\bar{\sigma}_i} \rangle_0 G_-[\hat{c}_{\sigma_i, j}, \hat{c}_{\sigma_f}^\dagger]. \quad (8)$$

This approximation becomes exact when the unperturbed state is fully spin-polarized hence exact for the Néel product state. To deal with $G_-[\hat{\eta}_{\bar{\sigma}_i}^z \hat{c}_{\sigma_i, j}, \hat{c}_{\sigma_f}^\dagger]$ more accurately and generically, we will need to consider the parent state with spatial spin entanglement, i.e. as a partially polarized, superposition of the two degenerate AFM states. We leave that for the future.

To the simplest but reasonable approximations and after eliminating $G_-[\hat{v}_{\sigma_i}, \hat{c}_{\sigma_f}^\dagger]$, we have

$$\begin{aligned} \left(\omega^2 - \frac{U^2}{4} \right) G_-[\hat{c}_{\sigma_i}, \hat{c}_{\sigma_f}^\dagger] &+ \sum_j t_{ij} (\omega - \sigma_i \langle \hat{s}_i^z \rangle_0) U \\ \times G_-[\hat{c}_{\sigma_i, j}, \hat{c}_{\sigma_f}^\dagger] &= (\omega - \sigma \langle \hat{s}_i^z \rangle_0) \delta_{x_i, x_f} \delta_{\sigma_i, \sigma_f}, \end{aligned} \quad (9)$$

where we used $\langle \hat{\eta}_{\bar{\sigma}_i}^z \rangle = -\sigma_i \langle \hat{s}_i^z \rangle$. Note that from here on, we drop the $_0$ index and promote $\langle \hat{s}_i^z \rangle$ to be a self-consistent state parameter.

Finally, a spatial-momentum Fourier transform (FT) makes the equation invertible by expressing $\langle \hat{s}_i^z \rangle = m_z e^{i\mathbf{x}_i \cdot \vec{Q}}$ with $\vec{Q} = (\pi, \pi)$:

$$\begin{aligned} (\omega^2 - U^2/4 - \omega \epsilon_{\mathbf{k}_i}) G_-[\hat{c}_{\sigma_i \mathbf{k}_i}, \hat{c}_{\sigma_f \mathbf{k}_f}^\dagger] \\ - U m_z \epsilon_{\mathbf{k}_i - \vec{Q}} G_-[\hat{c}_{\sigma_i \mathbf{k}_i - \vec{Q}}, \hat{c}_{\sigma_f \mathbf{k}_f}^\dagger] \\ = (\omega - \sigma_i m_z U) \delta_{\mathbf{k}_i, \mathbf{k}_f} \delta_{\sigma_i, \sigma_f}. \end{aligned} \quad (10)$$

Eliminating \mathbf{k}_f and keeping only diagonal spin indices, we find the \vec{Q} zone-folding equations for $G_-[\hat{c}_{\sigma \mathbf{k}}, \hat{c}_{\sigma \mathbf{k}}^\dagger]$. Let $G_-[\hat{c}_{\sigma \mathbf{k}}, \hat{c}_{\sigma \mathbf{k}}^\dagger] = G_{kk}$, $G_-[\hat{c}_{\sigma_i \mathbf{k} - \vec{Q}}, \hat{c}_{\sigma \mathbf{k}}^\dagger] = G_{Qk}$, $G_-[\hat{c}_{\sigma_i \mathbf{k} - \vec{Q}}, \hat{c}_{\sigma \mathbf{k} - \vec{Q}}^\dagger] = G_{QQ}$. We also use the square lattice nn bare dispersion $\epsilon_{\mathbf{k}} = -2t(\cos k_x + \cos k_y)$ which satisfies $\epsilon_{\mathbf{k} + \vec{Q}} = -\epsilon_{\mathbf{k}}$. Note that the sign-changing behavior would be spoiled if other hopping terms are included. Finally, we have

$$\begin{aligned} \begin{pmatrix} \omega^2 - U^2/4 - \omega \epsilon_{\mathbf{k}} & -U m_z \epsilon_{\mathbf{k}} \\ U m_z \epsilon_{\mathbf{k}} & \omega^2 - U^2/4 + \omega \epsilon_{\mathbf{k}} \end{pmatrix} \\ \times \begin{pmatrix} G_{kk} & G_{kQ} \\ G_{Qk} & G_{QQ} \end{pmatrix} = \begin{pmatrix} \omega - \sigma_i m_z U & 0 \\ 0 & \omega - \sigma_i m_z U \end{pmatrix} \end{aligned} \quad (11)$$

which is inverted to give

$$G_-[\hat{c}_{\sigma \mathbf{k}}, \hat{c}_{\sigma \mathbf{k}}^\dagger] = \frac{(\omega - \sigma m_z U/2) (\omega^2 - U^2/4 - \epsilon_{\mathbf{k}} \omega)}{(\omega^2 - U^2/4)^2 - \epsilon_{\mathbf{k}}^2 (\omega^2 - m_z^2 U^2)}. \quad (12)$$

To enforce the \vec{Q} zone-folding, we transform $\epsilon_{\mathbf{k}} = -2t(\cos k_x + \cos k_y) \rightarrow -2t(\cos(k_x + k_y) + \cos(k_x - k_y))$. After the transformation, we identifies G_{kk} with G_{QQ} , which is the GF between the same sublattices up to a spin-flip transition. $G_{kQ} = G_{Qk}$ is the GF between

different sublattices. Note that in the final expression Eq. (12) we have restored all m_z so that we can treat it as a self-consistent equation which would allow us to determine the state parameters. In this case, we only have a single parameter m_z .

Applications.— With Eq. (12), we study and discuss various major aspects of AFM Mott insulators which observed both experimentally and numerically.

The Mott Gap.— First of all, we obtain four dispersive upper or lower Hubbard bands from the poles of Eq. (12):

$$\omega_{0,i} = \pm \frac{U}{2} \sqrt{1 + \tilde{\epsilon}_{\mathbf{k}}^2 \pm |\tilde{\epsilon}_{\mathbf{k}}| \sqrt{\tilde{\epsilon}_{\mathbf{k}}^2 + 2(1 - 4m_z^2)}}, \quad (13)$$

where $\tilde{\epsilon}_{\mathbf{k}} = \sqrt{2}\epsilon_{\mathbf{k}}/U$ is a dimensionless, renormalized bare band dispersion. To extract the direct Mott gap, we can expand the dispersion Eq. (13) in the large- U limit, which yields $\omega_{0,i} \simeq \pm(U/2 - \sqrt{1 - 4m_z^2}\epsilon_{\mathbf{k}}/2)$. The band gap is minimal at $\epsilon_{\mathbf{k}} = W$ where W is the half bandwidth. For HM on the 2D square lattice with only nn hopping, $W = 4t$. Therefore, we find the Mott gap is $\Delta_{\text{Mott}} = U - \sqrt{1 - 4m_z^2} W$. The gap size increases with the AFM moment m_z . Such antiferromagnetism induced gap increasing is known as the magnetic blueshift for Mott insulators[30–34], which were observed both experimentally and numerically. Our results give the blueshift of the Mott gap due to AFM order to be $\Delta_{bs} = \Delta_{\text{AFM}} - \Delta_{\text{Param}} = (1 - \sqrt{1 - 4m_z^2}) W$. We immediately find it indeed increases m_z , in agreement with both numerical calculations and experimental observations.

Self-consistent solution.— With the lattice GF Eq. (12), we can compute m_z according to $\langle \hat{s}_i^z \rangle = \langle \eta_{\sigma i} \rangle = \langle [\hat{c}_{\sigma i}, \hat{c}_{\sigma i}^\dagger] \rangle / 2 = (1/2) i G_- [\hat{c}_{\sigma i}, \hat{c}_{\sigma i}^\dagger](t=0) = -(1/2) \int d^2k (2\pi)^{-2} \Im m[G_- [\hat{c}_{\sigma \mathbf{k}}, \hat{c}_{\sigma \mathbf{k}}^\dagger]]$. Without actually carrying out the \mathbf{k} -integral, we can expand Eq. (12) first and check the sum rule. We find a self-consistent equation $m_z = \int d^2k (2\pi)^{-2} (m_z - m_z/U + f(m_z^2))$. So, to the linear order, we do find that m_z decreases with decreasing U and the higher order terms allow us to obtain a self-consistent solution for m_z . We numerically solve the self-consistent equation and plot m_z in Fig. 1(a). Therefore, m_z only reaches the result of AFM Heisenberg model value[35] in the $U \rightarrow \infty$ limit. At finite U , we obtain an additional $1/U$ correction on top of that.

Local density of states.— We plot the spin projected local density of states (LDOS), partly also to illustrate the Mott gap blueshift, which agree well with cluster dynamical mean field results in Ref. [32]. Here we manually set the magnetization all the way down to $m_z = 0.1$ to exemplify the blueshift effect and the spectral imbalance, although such low magnetization regime is not accessible from the self-consistent solution.

Dispersion and spectral weights of Hubbard bands.— To carefully examine the properties of the Hubbard

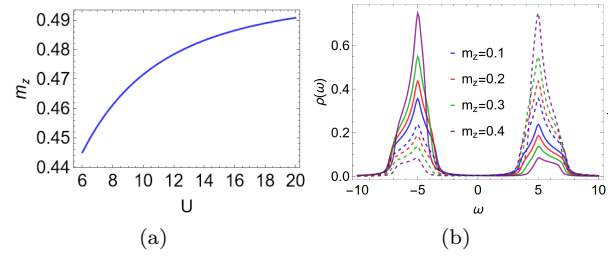


Figure 1. **1(a)** Self-consistent solution to magnetization. Here only single-particle charge fluctuation is taken into account, thus the deviation from full polarization is small. **1(b)** Spin projected local density of states at different magnetization. The solid line is for spin up and the dashed line is for spin down. To exemplify the blueshift effect and the spectral imbalance, we show results for m_z down to 0.1 beyond the self-consistent results.

bands, we rewrite Eq. (12) in terms of the poles $\omega_{0,i}(\mathbf{k})$ and their corresponding weights $\mathcal{W}_i(\mathbf{k})$:

$$\begin{aligned} G_-[\hat{c}_{\sigma \mathbf{k}}, \hat{c}_{\sigma \mathbf{k}}^\dagger](\omega, \mathbf{k}) &= \sum_i \frac{\mathcal{W}_i(\mathbf{k})}{\omega - \omega_{0,i}(\mathbf{k})} \\ &= \sum_i \frac{A_i(\mathbf{k})}{\omega - \omega_{0,i}(\mathbf{k}) + i0^+} + \frac{B_i(\mathbf{k})}{\omega - \omega_{0,i}(\mathbf{k}) - i0^+}. \end{aligned} \quad (14)$$

We find that $\mathcal{W}_i(\mathbf{k})$ is not a positive-definite function. This is because $G_-[\hat{c}_{\sigma \mathbf{k}}, \hat{c}_{\sigma \mathbf{k}}^\dagger](\omega, \mathbf{k})$ is a time-ordered GF, containing both retarded and advanced parts. $\text{sgn}(\mathcal{W}_i)$ automatically distinguishes between the retarded and advanced parts. Therefore, in the second line of Eq. (14), we choose $A_i = \Theta(\mathcal{W}_i)\mathcal{W}_i$, $B_i = \Theta(-\mathcal{W}_i)(-\mathcal{W}_i)$, in accordance with conventional notations so that both A_i and B_i are positive-definite functions. Thus the experimentally relevant spectral function $\mathcal{A}(\omega, \mathbf{k})$ is given as: $\mathcal{A}(\omega, \mathbf{k}) = i(G^R - G^A) = \sum_i \delta(\omega - \omega_{0,i}(\mathbf{k})) (A_i(\mathbf{k}) + B_i(\mathbf{k}))$.

We plot $\mathcal{A}(\omega, \mathbf{k})$ numerically in Fig. 2. We first show a generic momentum distribution curve (MDC) along high symmetry directions $(0,0) \rightarrow (0,\pi) \rightarrow (\pi,\pi) \rightarrow (0,0)$ for $m_z = 0.45$ in 2(a), then the extreme case for $m_z = 0.49$ in 2(b). 2(b) showcase the interesting limit where the fully polarized local moments turn one of the LHB into an exact flat band. We plot constant energy cuts at $\omega = -U/2 + \delta\omega$ with $\delta\omega \in \{1.5t, t, 0.5t, 0.2t, 0.1t, -0.2t\}$, from left to right, at $m_z = 0.45$. In all plots we set $U = 10t$ and $t = 1$. Recent ARPES studies on the parental compounds revealed nontrivial dispersion of the lower Hubbard bands[36]. Our results at $\delta\omega = -U/2 + 0.2t$ provides an explanation for the two ‘‘Fermi surface sheets’’ observed.

Discussion and Conclusion.— In this study, we establish a comprehensive theoretical framework to study the Antiferromagnetic Mott (AFM) states within the Hubbard model. We analytically derived the single-particle

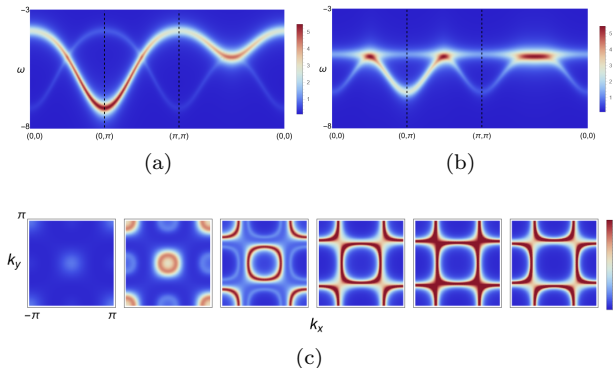


Figure 2. **2(a)** MDC for $m_z = 0.45$. **2(b)** MDC at $m_z = 0.49$. Both are plotted along high symmetry directions $(0,0) \rightarrow (0,\pi) \rightarrow (\pi,\pi) \rightarrow (0,0)$. **2(c)** Constant energy cuts at $\omega = -U/2 + \delta\omega$ with $\delta\omega \in \{1.5t, t, 0.5t, 0.2t, 0.1t, -0.2t\}$, from left to right, for $m_z = 0.45$. **2(b)** showcase the interesting limit where the fully polarized local moments turn one of the LHB into an exact flat band. **2(c)** is comparable to ARPES observations of Ref. [36]. Plot for $\delta\omega = -U/2 + 0.2t$ provides an explanation for the two "Fermi surface sheets" observed.

Green's functions (GFs) for the AFM Mott phase of the Hubbard model. Through the analysis of the GFs, we accounted for various important aspects of AFM Mott insulators which were established both numerically and experimentally. The Mott gap function explained the so called magnetic blueshift of the Mott gap. The spectral functions matches recent angle resolved photon emission (ARPES) experiments on the parental compounds of the cuprate high T_c superconductors. The remarkable alignment between our analytic theory and observations by both numerics and experiments proves that our comprehension of AFM Mott insulators is on the right track, and more importantly, provides a solid ground for further investigations on the doped AFM Mott insulators. Such alignment also demonstrates the validity and efficiency of the recently proposed algebraic dynamical theory framework[20], which underlies the construction of this work.

The analytic expression of the single-particle GFs for AFM Mott insulators unambiguously demonstrates previously proposed important characters of the large- U Hubbard model even away from half-filling. First, the expression clearly possesses nontrivial Luttinger surfaces or exact zeros, in addition to the atomic limit ones at $\omega = \sigma m_z U/2$. The nontrivial ones are given by the solutions of $\omega^2 - U^2/4 - \epsilon_k \omega = 0$, which clearly disperses. Secondly, the spectral weights vary strongly with both ω and \mathbf{k} . While this is observed by ARPES for a long time, theoretical understanding for such behavior is still difficult, especially for microscopic theories. It is previous found in ECFL[37] calculations for the 2D t - J model and in the unrealistic Hatsugai-Kohmoto model[38]. Finally,

the explicit Hubbard band dispersion make it possible to study topological states of large- U Hubbard models more precisely.

In conclusion, our work represents a substantial step forward in the theoretical treatment of AFM Mott states and laying a solid foundation for further exploration of the mechanism of high T_c superconductivity as doped AFM Mott insulators via the current framework.

Acknowledgement.— W.D. was supported by the National Key R&D Program of the MOST of China under Grant No. 2022YFA1602603 and the Startup Grant No. S020118002/002 of Anhui University. R.Y. was supported by the National Science Foundation of China under Grant No. 12334008 and 12174441.

-
- [1] J. G. Bednorz and K. A. Müller, Possible High T_C Superconductivity in the Ba-La-Cu-O System, *Zeitschrift für Physik B: Condensed Matter* **64**, 189 (1986).
 - [2] J. Zaanen, G. a. Sawatzky, and J. W. Allen, Band gaps and electronic structure of transition-metal compounds, *Phys. Rev. Lett.* **55**, 418 (1985).
 - [3] P. A. Lee, N. Nagaosa, and X.-G. Wen, Doping a Mott insulator: Physics of high-temperature superconductivity, *Rev. Mod. Phys.* **78**, 17 (2006), arXiv:0410445 [cond-mat].
 - [4] J. Hubbard, Electron correlations in narrow energy bands, *Proceedings of the Royal Society of London. Series A. Mathematical and Physical Sciences* **276**, 238 (1963).
 - [5] D. P. Arovas, E. Berg, S. A. Kivelson, and S. Raghu, The Hubbard model, *Annu. Rev. Condens. Matter Phys.* **13**, 239 (2022).
 - [6] P. W. Anderson, Antiferromagnetism. theory of superexchange interaction, *Physical Review* **79**, 350 (1950).
 - [7] G. Kotliar and A. E. Ruckenstein, New functional integral approach to strongly correlated fermi systems: the gutzwiller approximation as a saddle point, *Phys. Rev. Lett.* **57**, 1362 (1986).
 - [8] S. Florens and A. Georges, Quantum impurity solvers using a slave rotor representation, *Phys. Rev. B* **66**, 165111 (2002).
 - [9] D. Yoshioka, Slave-fermion mean field theory of the hubbard model, *J. Phys. Soc. Japan* **58**, 1516 (1989).
 - [10] X.-J. Han, C. Chen, J. Chen, H.-D. Xie, R.-Z. Huang, H.-J. Liao, B. Normand, Z. Y. Meng, and T. Xiang, Finite-temperature charge dynamics and the melting of the mott insulator, *Physical Review B* **99**, 245150 (2019).
 - [11] W. Ding, R. Yu, Q. Si, and E. Abrahams, Effective exchange interactions for bad metals and implications for iron-based superconductors, *Phys. Rev. B* **100**, 235113 (2019).
 - [12] C. Ye, P. Cai, R. Yu, X. Zhou, W. Ruan, Q. Liu, C. Jin, and Y. Wang, Visualizing the atomic-scale electronic structure of the ca2cuo2cl2 mott insulator, *Nat. Commun.* **4**, 1365 (2013), arXiv:1201.0342.
 - [13] W. Ding and Q. Si, Local density of states induced near impurities in mott insulators, *arXiv* (2018), arXiv:1810.03309 [cond-mat.str-el].
 - [14] P. Cai, W. Ruan, Y. Peng, C. Ye, X. Li, Z. Hao,

- X. Zhou, D.-H. Lee, and Y. Wang, Visualizing the evolution from the mott insulator to a charge-ordered insulator in lightly doped cuprates, *Nat. Phys.* **12**, 1047 (2016), [arXiv:1508.05586 \[cond-mat.supr-con\]](#).
- [15] F. C. Zhang and T. M. Rice, Effective hamiltonian for the superconducting Cu oxides, *Phys. Rev. B* **37**, 3759 (1988).
- [16] B. S. Shastry, Extremely correlated fermi liquids, *Phys. Rev. Lett.* **107**, 056403 (2011).
- [17] B. S. Shastry, Extremely correlated fermi liquids: the formalism, *Phys. Rev. B* **87**, 125124 (2013).
- [18] R. Žitko, D. Hansen, E. Perepelitsky, J. Mravlje, A. Georges, and B. S. Shastry, Extremely correlated fermi liquid theory meets dynamical mean-field theory: Analytical insights into the doping-driven mott transition, *Phys. Rev. B* **88**, 235132 (2013), [arXiv:1309.5284](#).
- [19] P. Mai, S. R. White, and B. S. Shastry, t - t' - j model in one dimension using extremely correlated fermi-liquid theory and time-dependent density matrix renormalization group, *Phys. Rev. B* **98**, 035108 (2018).
- [20] W. Ding, Algebraic-dynamical theory for quantum many-body hamiltonians: A formalized approach to strongly interacting systems, [arXiv:2202.12082 10.48550/ARXIV.2202.12082](#) (2022).
- [21] J. Schwinger, Unitary operator bases, *Proceedings of the National Academy of Sciences* **46**, 570 (1960).
- [22] U. Fano, Description of states in quantum mechanics by density matrix and operator techniques, *Rev. Mod. Phys.* **29**, 74 (1957).
- [23] A. O. Barut and A. Böhm, Dynamical groups and mass formula, *Physical Review* **139**, B1107 (1965).
- [24] I. Dzyaloshinskii, Some consequences of the luttinger theorem: the Luttinger surfaces in non-fermi liquids and mott insulators *Phys. Rev. B* **68**, 085113 (2003).
- [25] K. B. Dave, P. W. Phillips, and C. L. Kane, Absence of luttinger's theorem due to zeros in the single-particle green function, *Phys. Rev. Lett.* **110**, 090403 (2013).
- [26] S. Pairault, D. Sénéchal, and A.-M. Tremblay, Strong-coupling perturbation theory of the hubbard model, *Eur. Phys. J. B* **16**, 85 (2000).
- [27] S. Pairault, D. Sénéchal, and A.-M. S. Tremblay, Strong-Coupling Expansion for the Hubbard Model, *Phys. Rev. Lett.* **80**, 5389 (1998).
- [28] J. Schwinger, Unitary transformations and the action principle, *Proceedings of the National Academy of Sciences* **46**, 883 (1960).
- [29] D. R. Hartree, The wave mechanics of an atom with a non-coulomb central field. part i. theory and methods, *Mathematical Proceedings of the Cambridge Philosophical Society* **24**, 89 (1928).
- [30] K. W. Blazey and H. Rohrer, Antiferromagnetic phase diagram and magnetic band gap shift of NaCrS₂, *Physical Review* **185**, 712 (1969).
- [31] X. Wang, E. Gull, L. de' Medici, M. Capone, and A. J. Millis, Antiferromagnetism and the gap of a mott insulator: Results from analytic continuation of the self-energy, *Physical Review B* **80**, 045101 (2009).
- [32] L. Fratino, P. Sémon, M. Charlebois, G. Sordi, and A.-M. S. Tremblay, Signatures of the mott transition in the antiferromagnetic state of the two-dimensional hubbard model, *Physical Review B* **95**, 235109 (2017).
- [33] M. Hafez-Torbati, D. Bossini, F. B. Anders, and G. S. Uhrig, Magnetic blue shift of mott gaps enhanced by double exchange, *Physical Review Research* **3**, 043232 (2021).
- [34] M. Hafez-Torbati, F. B. Anders, and G. S. Uhrig, Simplified approach to the magnetic blue shift of mott gaps, *Phys. Rev. B* **106**, 205117 (2022).
- [35] A. W. Sandvik, Finite-size scaling of the ground-state parameters of the two-dimensional heisenberg model, *Physical Review B* **56**, 11678 (1997).
- [36] C. Hu, J.-F. Zhao, Y. Ding, J. Liu, Q. Gao, L. Zhao, G.-D. Liu, L. Yu, C.-Q. Jin, C.-T. Chen, Z.-Y. Xu, and X.-J. Zhou, Evidence for multiple underlying Fermi surface and isotropic energy gap in the cuprate parent compound Ca₂CuO₂Cl₂, *Chinese Phys. Lett.* **35**, 067403 (2018).
- [37] P. Mai and B. S. Shastry, Extremely correlated Fermi liquid of the $t - J$ model in two dimensions, *Phys. Rev. B* **98**, 205106 (2018).
- [38] Y. Hatsugai and M. Kohmoto, Exactly solvable model of correlated lattice electrons in any dimensions, *Journal of the Physical Society of Japan* **61**, 2056 (1992).